ROLE OF DELAYED FEEDBACK AND GRAPHENE SATURABLE ABSORBER IN CAVITY SOLITON

A thesis submitted in the partial fulfillment of the requirements for the award of

degree of

Master of Science

in

Physics

Submitted by

Ramanpreet Kaur

Rollno.301704027

Under the supervision of

Dr.Soumendu Jana

(Associate Professor)

SCHOOL OF PHYSICS AND MATERIAL SCIENCE

THAPAR INSTITUTE OF ENGINEERING AND TECHNOLOGY

Patiala-147001,Punjab,INDIA

July 2019

I dedicate my thesis to my loving parents Mr. Bhagwant Singh and Mrs. Baljinder Kaur, friends and my elder brother Gaganjot Singh who have always been supportive toward me.

CERTIFICATE

I hereby certify that the work which has been presented in this thesis entitled, **"Role of delayed feedback and graphene saturable absorber in cavity soliton"**, Submitted in partial fulfillment of the requirements for the award of degree of **Master of Science in Physics** at **Thapar Institute of Engineering and Technology, Patiala**, is an authentic record of my own work carried out under the supervision of **Dr. Soumendu Jana**, Associate Professor, School of Physics and Materials Science and refers other researcher's work which are duly listed in reference section. The matter embodied in this thesis has not been submitted for the award of any other degree of this or any other university.

Ramanpreet

(Ramanpreet Kaur)

Roll number:301704027

Date: 15 July, 2019

Place: Patiala

This is to certify that the above statement made by the candidate is correct and true to the best of my knowledge.

Soumendu Jana

DR.SOUMENDU JANA

Associate Professor

School of Physics and Materials Science

TIET, Patiala

ACKNOWLEDGEMENT

I would like to express my deepest gratitude to my supervisor **Dr.Soumendu Jana** for excellent guidance, caring and patience. He let me experience the research, patiently corrected my writing and supported my research. I could not have imagined having a better advisor and mentor than him for my thesis.

I would like to thank **Dr.O.P.Pandey,** Professor and Head, School of Physics and Materials Science for his support and providing me with an excellent atmosphere for doing research. Special thanks to the staff at the School of Physics and Materials Science for providing me a friendly atmosphere and encouraging me throughout this work.

I would also like to thank my parents and my younger brother for supporting me and encouraging me with their best wishes.

Above all I render my gratitude to the Almighty who bestowed me with the strength and vision to walk on the path of truth.

Date: 15 July, 2019

Ramanpreet

Ramanpreet Kaur

INDEX

Chapter-1

Introduction

Chapter-II

CAVITY SOLITON WITH DIFFERENT FEEDBACK AND SATURABLE ABSORBER

Chapter-III

ABSTRACT

The formation of localized structure in wide area nonlinear cavity has been investigated. Analytical as well as numerical methods have been adopted to determine the evolution of the localized structures. Cavity soliton have been generated with different delayed feedback. The influence of delay is compared with the case of no delay in feedback. The phase portraits have been drawn and analyzed to identify the center of the localized structure, i.e., cavity soliton. The nonlasing zone has also been identified. The whole investigation on cavity soliton has been carried out in two parallel situations; with and without graphene saturable absorber. The influence of graphene has been identified. Applications of the result of the present investigation have been suggested.

CHAPTER-1

1.1 Introduction to Soliton

Soliton is a localized structure which may be wave or a beam or a pulse that maintains its initial shape and size during propagation even after the collision with another soliton [1-2]. It was first observed by John Scott Russell in 1834 in union canal in Glasgow and was reported by him after extensive research on it for nearly a decade [2]. He however mentioned it as a 'wave of translation'. With time the soliton has been emerged as a multidisciplinary research topic. For example, soliton can be found in major disciplines like, Physics, Chemistry, Biology and Biochemistry, electrical engineering, mechanical engineering [3-4]. It can be found in many interdisciplinary platforms too. Solitons are caused by the nonlinear optical effect. They grow due to the cancellation of dispersive effect/ (s) by the nonlinear effect/ (s) in the medium. For example, a pulse will broaden due to dispersion during propagation[4]. Now if the intensity of the pulse is very high (generally laser pulse is taken) it can create nonlinear polarization in the media through which it is propagating [5]. The nonlinear polarization in turn creates nonlinear refractive index. This intensity dependent refractive index, i.e., Kerr effect, will create self phase modulation (SPM). SPM induced pulse contraction may compensate group velocity dispersion (GVD) induced broadening and eventually leads to the formation of soliton [6]. Since this pulse is localized in time scale it is referred as temporal soliton. A soliton can be localized in space domain also and can be referred as spatial soliton[4]. For example, any beam will diverge due to self-diffraction. Kerr nonlinearity may lead to self-focusing of the beam. When these self-focusing balances the self-diffraction perfectly one can get a spatial soliton, which will not diverge of converge due to propagation[3]. At the primary stage the concept of soliton has been developed mostly in conservative systems, i.e., in a system wherein the total mass-energy is

conserved [1, 5]. But practical systems are not conserved ones. Getting soliton in practical systems was not very common in those days. With the advent of new techniques the research on soliton has been extended in many practical 'non-conservative' systems. Mathematically, solitons are the solutions of a weakly nonlinear dispersive partial differential equation that describes the dynamical system [4, 5]. A number of equations have been successfully used for exploring solitons; e.g., KdV equation, nonlinear Schrödinger equation, complex Ginzburg-Landau equations etc [5, 7, 8].

In conservative systems, the formation of soliton needs the dispersion-broadening to be balanced by the nonlinearity induced contraction. And this balance is sufficient. As long as this balance is maintained the soliton will be there [4]. But in case of non-conservative / dissipative systems, in addition to the aforesaid balance (between dispersion/ diffraction and nonlinearity) the system loss essentially to be compensated by an external gain [2]. That means a continuously energy flow is required for the maintenance of the soliton. Such solitons obtained in non-conservative/ dissipative media is called as dissipative solitons. Conservative solitons are formed in laboratory conditions, while dissipative solitons are formed in practical systems. There are many examples of naturally occurring solitons, which are dissipative. For example, the rolling cloud. A special type of dissipative soliton can be found in laser cavity and are classified as cavity soliton (CS) [1,2].

1.2Introduction to Cavity Soliton

Cavity Soliton is a kind of dissipative soliton that can be formed inside a semiconductor cavity. They are bi-stable soliton in nature [2]. It attracted research attention because of its potential to act like a 'bit of information' and so can be used in future optical memory devices or data storage devices. Cavity solitons are formed on the transverse cavity plane (perpendicular to the cavity

axis) in a nonlinear cavity [4]. These appear to be a collection of bright spot against dark background or dark spots present on a bright background as (shown in Fig.1.1).

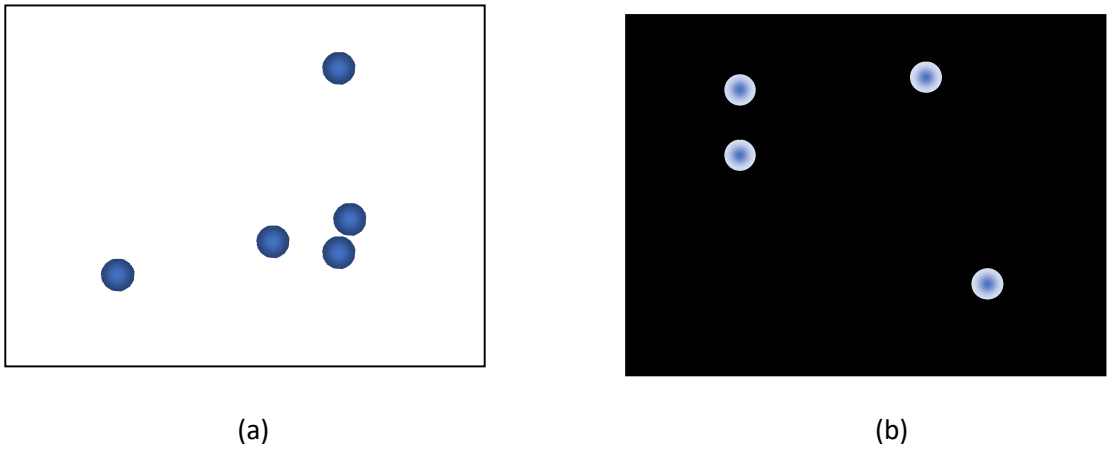

Fig.1.1. Typical appearance of cavity solitons: (a) bright spot against dark background and (b) dark spots present on a bright background

There are three essential conditions to be satisfied in case of a cavity soliton and those conditions are: (i) exponential localization (ii) bi-stability (iii) freedom of localization on any point on the transverse plane [1]. Some more features made CS very interesting. For example, CSs are self -localized but do not depend on any boundary conditions. CS can be independently controlled. This condition is very useful for all-optical processes [2]. They can present in various transverse locations of the transverse cavity plane. Also, CS can have motion, which can be applied for scanning purpose. CS is formed by the overlapping of a patterned state on a homogeneous stationary state [2, 3]. That's why CS research attracted researchers from various disciplines, who work on pattern formation too. The bistability of CS has an exclusive meaning. Depending on the initial conditions the CS can be present in one or more states with same controlling parameters at same time [2]. So it can be 'on' or 'off' in the same set of system parameters.

To form a CS a wide area cavity is required. Vertical cavity surface emitting laser (VCSEL) is an example of such system in which CSs are formed [9]. The wide area is also helpful to observe the drift or other motion of the CSs. The semiconductor systems (e.g., VCSEL) are preferred more than optical systems in order to observe the CS [9]. The reason behind is that the timescale of CS formation in the semiconductor materials is of the order of carrier recombination time [4]. This time is much smaller in comparison with the other macroscopic systems as it is of the order of several nanoseconds. The size of the CS is controlled by the diffraction length 'a'. $a = \alpha\sqrt{L\lambda F}$, where L is the cavity length, λ is the wavelength of light and F is the resonator finesse [10]. Optical pumping is very useful for obtaining the CS [11].

Theoretical research on CS combines the idea of solving nonlinear differential equation, stability analysis and nonlinear dynamics. There are only few methods to solve a nonlinear dynamical problem theoretically CS, like separation method [12], variation method [13]. These are analytical methods. Most of the theoretical investigations on CS are accomplished through numerical methods. In the current investigation we adopt complex Ginzburg landau equation (CGLE) to present our nonlinear dynamical system [14]. The CGLE is solved numerically by using split-step Fourier method (SSFM).

Feedback mechanism has a critical role in the formation of the CS. Earlier we mentioned that the system loss needs to be essentially compensated by an external gain. Here in our investigation the external gain is provided by a feedback mechanism [15]. Furthermore, depending on the feedback property the features of a CS will be varied. The feedback strength, feedback delay are very significant for the CS formation [14].

We investigate CS with delayed feedback as well as feedback without any delay. We also investigate CS with graphene as a saturable absorber in CGLE equation with and without delayed feedback [14, 15].

1.3 VCSEL

As we know that most of the cavity solitons forms in the nonlinear dissipative of VCSEL. VCSEL is a semiconductor laser developed in the mid 1980's [9]. It is of lower cost and reliable in terms of stable and consistent radiation. Its temperature tolerance is great. VCSEL has high output power and a longer operating lifetime. Besides, it requires low threshold current (~ few micro-ampere) and has low noise [10]. It is stable in nature and have uniform lasing wavelength. The VCSEL has very less temperature dependence due to which the wavelength of emitted radiation remains constant [7 9]. VCSELs work out up to temperature 80ºC without any major fluctuations in the radiation. The highest power that can be generated is of the order of 1200W/cm^2. VCSELs are much easier to manufacture than other lasers [5]. Due to the aforesaid features and its radiation profile and few more advantages (like, can be arrayed very easily, can be used in the local area networks advantageously) VCSEL are gradually replacing the edge emitting laser. VCSEL are fabricated by growing semiconductor layers on top of a substrate through molecular beam epitaxy method (which is also used for crystal growth) [7 9]. In VCSEL an active layer is sandwiched between the two mirrors, which are basically distributed Bragg reflectors (DBR) [7 9]. These DBR mirrors have an important property that is they are highly reflective in nature having reflectivity near about 99.5-99.9%. The DBR have an alternating low and high refractive index layers [7 9]. This causes the oscillation of light perpendicular to the semiconductor layers and eventually exits through the top mirror of the cavity device [16, 17]. Various methods have been developed to achieve a current detention to the active area. One of

the methods is etching, which is usually done on the top mirror [7]. Proton implantation method is the other option. This method is used for the fabrication of commercial scale VCSELs. Fig.1.2. shows the structure of typical VCSEL highlighting different layers.

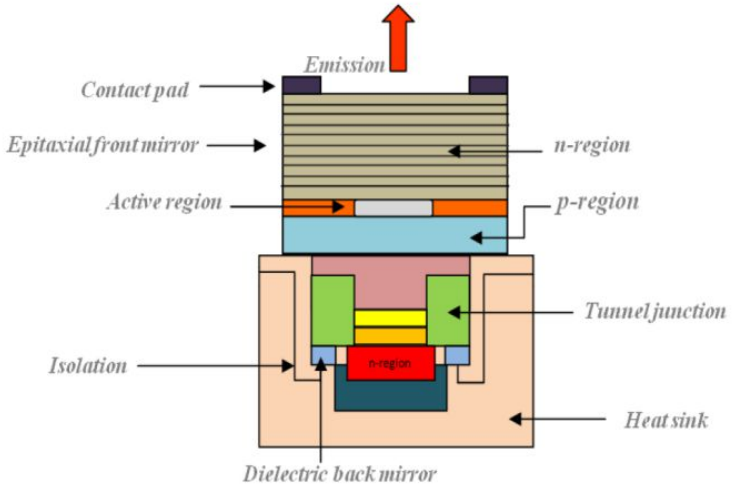

Fig.1.2: The structure of a typical VCSEL.

1.4 Graphene as a saturable absorber

Saturable absorber is a material wherein the absorption of light decreases with increase in the intensity of light. Most materials can show some saturable absorption, but usually only at very high intensities. It is so high that it may create an optical damage [10]. Saturable absorbers (SA) are very useful for the formation of CSs. The significant parameters for a saturable absorber are the wavelength range where it absorb, the dynamic response. i.e., how fast it recovers, the saturation intensity or fluence (i.e., at which intensity or pulse energy the material saturates) [9]. SA are widely used for passive Q- switching devices. For cavity soliton formation generally semiconductor SA mirrors (SESAM) are used. Recently, graphene has emerged as a significant SA. We used graphene as a saturable absorber because of its gapless energy band structure. Graphene is a strong conductor [9, 10]. The delocalized electrons that flow through the positively

charged carbon atoms are responsible for this. Graphene is very thin (~ one atom thick) and transparent. Also graphene has large surface area, good thermal and chemical stability, high conductivity and mechanical flexibility. For these qualities graphene and graphene-based materials have been widely used in energy storage devices, electrodes etc. Graphene can sustain a current density up to 1,000,000 times greater than that of copper and its intrinsic mobility is 1,000 times more than that of silicon. Moreover, thermal conductivity of graphene is significantly high

In our investigation graphene saturable absorber (GSA) is used in the anticipation to reduce the required feedback strength for generation of CS. Also, one can take (in principle) all the advantages of GSA for CS investigation. Also, the unique properties of GSA can be manipulated for improvement of the performance of the CS as well as to identify new feature of CSs.

1.5 Review on cavity soliton

The CS is a special type of dissipative soliton [13]. The CS theory has been developed on mainly three elegant theories. First is the standard soliton theory which portrays the formation of soliton by virtue of the balance between non-linearity and dispersion / diffraction [15]. Second is the theory of nonlinear dynamics (given by Poincare and many leading scientists) that gives the idea of the soliton dynamics, bifurcations etc. Third is the stability analysis. Since, CSs are formed in a dissipative system; they are localized in a place, which is far from equilibrium. Prigogine's ideas related to such far from equilibrium systems are useful for CS theory [14-15].

Like DS, a CS can have different shapes depending on the amount of energy which is supplied [1]. CSs are not decaying solutions. One of the most important spatial DS soliton is the cavity soliton. These are stable and are self-localized structures in a dissipative medium like a non-

linear optical cavity [3]. CSs are formed in a driven optical non-linear cavity. When soliton occurs in a driven non-linear cavity placed in front of the single feedback mirror it is called a feedback soliton. An example of cavity system that host spatial dissipative soliton is the VCSEL [9]. These are the semiconductor micro cavities enclosed by Bragg reflectors of high reflectivity. To provide gain to the system, quantum well structures are used as an active medium.

CSs have been excited in a VCSEL which is operated as an amplifier i.e., biased slightly below the lasing threshold value. CSs have been formed in three major configurations (i) VCSEL with holding and writing beam, (ii) VCSEL with frequency –selective feedback and (iii) VCSEL with SA. The second and third configurations need no external holding beam. Removal of the holding beam made the device simpler [10]. This also reduces the unwanted thermal effects and cross terms.

CSs are very sensitive to phase or intensity gradients of the intracavity field. In fact, any kind of gradient present in the cavity can influence the CS. Such gradient can set in a drift of CS across the transverse cavity plane [18, 19]. The dynamics of CSs were studied under the influence of a various generalized equations. To control the position of cavity solitons, the inhomogeneties in the system parameter can be used.

CSs have been proposed to have potential application for data storage, scanning etc. CS is generated in a VCSEL [13]. Now, VCSEL based 3D imaging has been developed in recent days [20]. We, in the current investigation, try to develop some basic concepts, which will be useful for 3D imaging with the help of CS in VCSEL. Following is the review on 3D imaging.

1.6 Motivation/Gap:

Feedback has an important role in the formation of CSs. Localized structures in cavity (and hence CSs) have been investigated with and without delay in feedback. But in those cavities graphene has not been used at all. Since the presence of graphene as a saturable absorber may significantly improve the system performance and /or may create new features in the CSs, it is worth to investigate CS formation with and without delayed feedback in VCSEL coupled with graphene saturable absorber. The knowledge of the effect of delayed feedback can be utilized for the 3D imaging purpose.

1.7 Objectives:

Our objectives of investigation are

- to generate cavity solitons in VCSEL coupled with graphene saturable absorber and a delayed feedback.
- to identify the effect of the delay in feedback on the generation of cavity solitons.

1.8 Methodology:

The complex Ginzburg-Landau equation (CGLE) plays an important role in modelling of various nonlinear dynamical systems, e.g., nonlinear optical waves, second-order phase transitions and even superconductivity [21]. CGLE is an amplitude equation that describe the onset of instability near an Andronov-Hopf bifurcation in a large area dynamical systems, e.g., the VCSEL cavity[16,17]. In nonlinear optics, equations from CGLE family are widely used, for example, in mode-locking lasers and ultra short pulse propagation in optical fiber or transmission lines. They

are the key equations for the study of multimode lasers dynamics [17]. Besides, they are widely used for investigating pattern formation in both nonlinear optical and non-optical media [16].

For our investigation we consider a cavity that comprises of a VCSEL coupled with feedback and graphene saturable absorber. The intra-cavity electric field dynamics can be mathematically presented by a cubic-quintic CGLE [17-18]. Actually, the saturable absorber term has been approximated and simplified to cubic-quintic terms. It can be viewed in this way: the cubic term try to increase, while the quintic term tends to decrease the saturation effect. By the interplay of the two counteracting terms the absorption eventually saturates [8]. We take one-dimensional cubic-quintic CGLE for the complex amplitude $A(x,t)$ of the intra-cavity field in VCSEL with delayed feedback as follows [14]:

$$\partial_t A = \left(\beta + \frac{\iota}{2}\right)\partial_{xx}A + \delta A + (\epsilon + \iota)|A|^2 A + (\mu + \iota\nu)|A|^4 A + \eta e^{\iota\psi} A(x, t-\tau) \qquad (1)$$

The term in the LHS describes the evolution of the cavity field. In the RHS, the parameter β>0 is the diffusion coefficient; second-order dispersion (diffraction) is scaled to ½. δ is the linear loss or gain parameter. The third and forth terms arise due to cubic and quintic effects respectively [18]. The parametersϵ, μ, and ν determine the profile of the nonlinearity. In the third and forth terms the real parts lead to cubic and quintic nonlinearities respectively, while the imaginary parts represent nonlinear losses (or gain, depending on the sign) [16]. The last term actually counts for the delayed feedback, while τ being the delay.

When we add graphene as a saturable absorber in the cavity the CGLE is modified as follows:

$$\partial_t A = \left(\beta + \frac{\iota}{2}\right)\partial_{xx}A + \delta A + \alpha_{ns} A + (\epsilon + \iota) g|A|^2 A + (\mu + \iota\nu) g^2 |A|^4 A + \eta e^{\iota\psi} A(x, t-\tau) \quad (2)$$

We take two different cases: one is CGLE with delayed feedback and the other is CGLE equation without delayed feedback. By reduce each CGLE into three ordinary differential

equations which further gives 3D plots that show the CS formation region [21]. Then we repeat the process for both the feedback conditions using graphene as a saturable absorber in CGLE. Delayed feedback may play an important role in 3D imaging.

CHAPTER 2

2.1 CS WITH DELAYED FEEDBACK:

We consider the following CGLE with delayed feedback: (actually the eq.1)

$$\partial_t A = \left(\beta + \frac{\iota}{2}\right)\partial_{xx}A + \delta A + (\epsilon + \iota)|A|^2 A + (\mu + \iota\nu)|A|^4 A + \eta e^{\iota\psi} A(x, t-\tau) \qquad (3)$$

We follow the method stated by N. N. Rosanov in ref. [6]. Let us start with the case of stationary structures where the field envelope depends on the evolution variable harmonically. Now, we put $A = Fe^{-i\alpha t}$

The complex amplitude F depends only on D co-ordinates$(x_1, x_2, x_3, \dots\dots, x_D)$.

Then it follows from CGLE equation with delayed feedback as:

$$\frac{\partial}{\partial t}(Fe^{-\iota\alpha t}) = \left(\beta + \frac{\iota}{2}\right)\frac{\partial^2}{\partial x^2}(Fe^{-\iota\alpha t}) + \delta\left(Fe^{-i\alpha t}\right) + (\epsilon + i)\left|Fe^{-i\alpha t}\right|^2 Fe^{-\iota\alpha t}$$
$$+ (\mu + \iota\nu)|Fe^{-\iota\alpha t}|^4 Fe^{-\iota\alpha t} + \eta e^{\iota\psi} Fe^{-\iota\alpha t}(x, t-\tau)$$

Now after simplifying this equation and taking $e^{-\iota\alpha t}$ part common and canceling out from both sides we lead to following equation as shown below:

$$-F\iota\alpha(e^{-\iota\alpha t}) = e^{-\iota\alpha t}\left[\left(\beta + \frac{\iota}{2}\right)\partial_{xx}F + \delta F + (\epsilon + \iota)|F|^2 F + (\mu + \iota\nu)|F|^4 F + \eta e^{\iota\psi} F(x, t-\tau)\right]$$

Now dividing whole equation by $\left(\beta + \frac{\iota}{2}\right)$ we get

$$(2\beta + \iota)\frac{d^2F}{dr^2} + \frac{(D-1)}{r}\frac{dF}{dr}(2\beta + \iota) + 2F(\iota\alpha + \delta + (\epsilon + \iota)|F|^2 + (\mu + \iota\nu)|F|^4 + \eta e^{\iota\psi}(x, t$$
$$- \tau) = 0$$

By separating real and imaginary parts, we get further two equations:

$$\frac{d^2F}{dr^2}+\frac{(D-1)}{r}\frac{dF}{dr}(2\beta)+2F(\delta+\epsilon)|F|^2+\mu|F|^4+2FRe\left[\eta e^{\iota\psi}(x,t-\tau)\right]=0 \quad (4)$$

And $$\frac{d^2F}{dr^2}+\frac{(D-1)}{r}\frac{dF}{dr}+2F\left[\alpha+|F|^2+\nu|F|^4+Im(\eta e^{\iota\psi}(x,t-\tau)\right]=0 \quad (5)$$

Now putting $F=Ae^{\iota\phi_0}$ in equations (4)and (5) and further simplifying by taking derivatives we get again two equations:-

$$\frac{dK}{dr}-\frac{KQ}{\beta}-Q^2-\frac{1}{2\beta}\frac{dQ}{dr}+\frac{(D-1)}{r}\left[K-\frac{Q}{2\beta}\right]+\frac{1}{\beta}(\delta+\epsilon A^2+\mu A^4+[\eta\cos(\psi-\omega\tau)]=0 \quad (6)$$

And

$$\frac{dK}{dr}+4\beta KQ+2\beta\frac{dQ}{dr}-Q^2+\frac{(D-1)}{r}(K+2\beta Q)+2[\alpha+A^2+\nu A^4+\eta\sin(\psi-\omega\tau)]=0 \quad (7)$$

Here,$K=\frac{1}{\mathrm{A}}\frac{dA}{dr}$.

These two equations are added and subtracted to give rise to the following two equations:-

$$\frac{dK}{dr}=Q^2-\frac{(D-1)K}{r}-\frac{2}{\left(2\beta+\frac{1}{2\beta}\right)}\left[\delta+\epsilon A^2+\mu A^4+[\eta\cos(\psi-\omega\tau)]\right]-\frac{1}{\beta\left(2\beta+\frac{1}{2\beta}\right)}\left[\alpha+A^2+\nu A^4+\right.$$

$$\left.[\eta\sin(\psi-\omega\tau)]\right]=0 \quad (8)$$

And

$$\frac{dQ}{dr}=-2KQ-\frac{(D-1)}{r}Q+\frac{2}{(4\beta^2+1)}[\delta+\epsilon A^2+\mu A^4+\eta\cos(\psi-\omega\tau)]+\frac{4\beta}{(4\beta^2+1)}[\alpha+A^2+\nu A^4+$$

$$\eta\sin(\psi-\omega\tau)] \quad (9)$$

Now finally we get three coupled ordinary differential equations as follows:

$$\frac{dA}{dr}=\mathrm{KA} \quad (10)$$

$$\frac{dK}{dr} = Q^2 - \frac{(D-1)K}{r} - \frac{2}{\left(2\beta+\frac{1}{2\beta}\right)}[\delta + \epsilon A^2 + \mu A^4 + \eta cos(\psi - \omega\tau)] - \frac{1}{\beta\left(2\beta+\frac{1}{2\beta}\right)}[\alpha + A^2 + \nu A^4 + \eta \sin(\psi - \omega\tau)] \quad (11)$$

$$\frac{dQ}{dr} = -2KQ - \frac{(D-1)}{r}Q + \frac{2}{(4\beta^2+1)}[\delta + \epsilon A^2 + \mu A^4 + \eta \cos(\psi - \omega\tau)] + \frac{4\beta}{(4\beta^2+1)}[\alpha + A^2 + \nu A^4 + \eta \sin(\psi - \omega\tau)] \quad (12)$$

Now, we solve the above three coupled differential equations (10-12) by Range-Kutta method (i.e., numerically). The result is described in the following paragraphs.

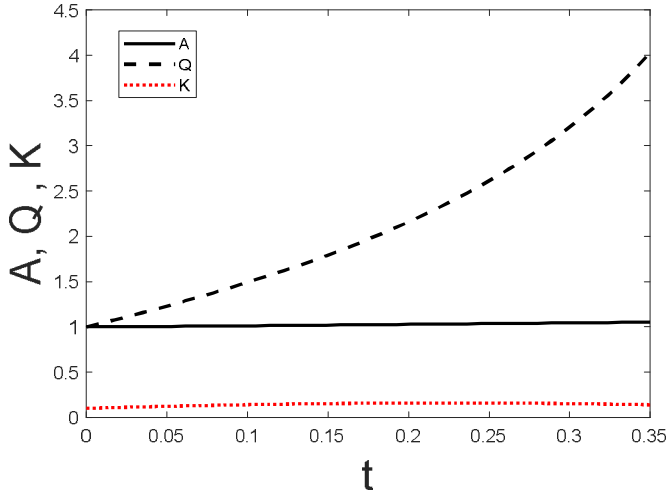

Fig.2.1: Evolution ofA, Q and K with t where parameters are β=6.2, α=0.7, ∈= 4.0 , μ=2, δ=0.51 ν=-0.1, η=0.2, Ψ=3.17, ω=9, τ=3.

Evolution of real amplitude(A), rate of change of real amplitude (K) and the rate of change of phase (Q) with t is presented in fig. 2.1. A And K remains constant while Q increases with t. This indicates the formation of a structure of constant amplitude but of changing phase. It can be

considered as a CS if its three major properties (mentioned earlier) are satisfied. The complex nonlinearity of the system may lead to such variation.

Now we plot the CS solution

The behaviour of A(r), Q(r) and K(r) is asymptotic for r→0 and r→infinity. Solution of quations (10-12) can be plotted in AKQ phase space. The 3D curves in Fig. 2.2 give the radial dependence of A, Q and K of the localized structure, i.e., the CS in the phase space AKQ. One end (point O) of the curve corresponds to the center of the localized structure and the other end (point NL) corresponding to the non lasing regime.

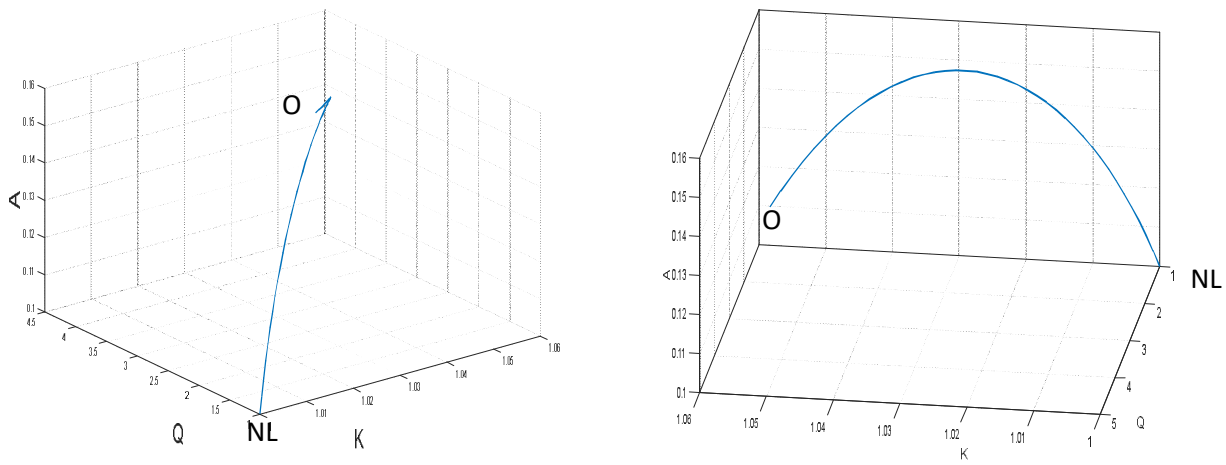

(a) (b)

Fig.2.2: Cavity soliton solution line in AQK space where all the parameters are same as Fig.2.1. (a) & (b) are in two different orientations. The points O and NL correspond to the center of CS and nonlasing zone respectively.

2.2 CS WITHOUT DELAYED FEEDBACK:

We now consider no delay in feedback by setting $\tau = 0$ (i.e., delayed term is zero). Rest of the parameters in all equation remain the same. Then we get the evolution *ofA,* Q and K as follows.

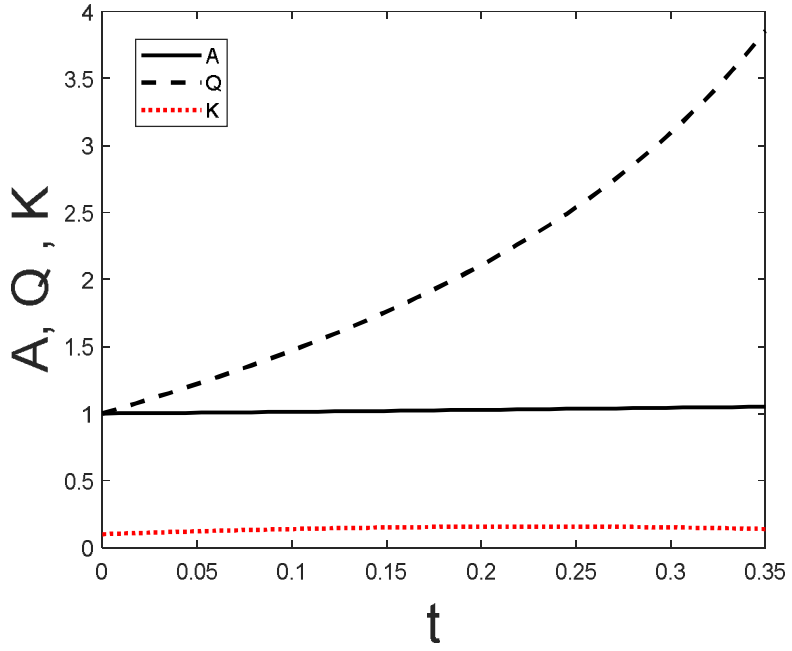

Fig.2.3: Evolution A, Q and K with t having parameters remains same as in above case except τ i.e., β=6.2, α=0.7, ϵ =4.0, μ=2, δ=0.51, v=-0.1, η=0.2, ψ=3.17, ω=9, τ=0.

Evolution of real amplitude(A), rate of change of real amplitude (K) and the rate of change of phase (Q) with t is presented in fig.2.3. A And K remain constant while Q increases with$t$. This indicates the formation of a structure of constant amplitude but of changing phase. Here the phase change is however bit smaller. It can be considered as a CS provided that its three major properties are satisfied. The corresponding CS solution in the AKQ phase space is as follows.

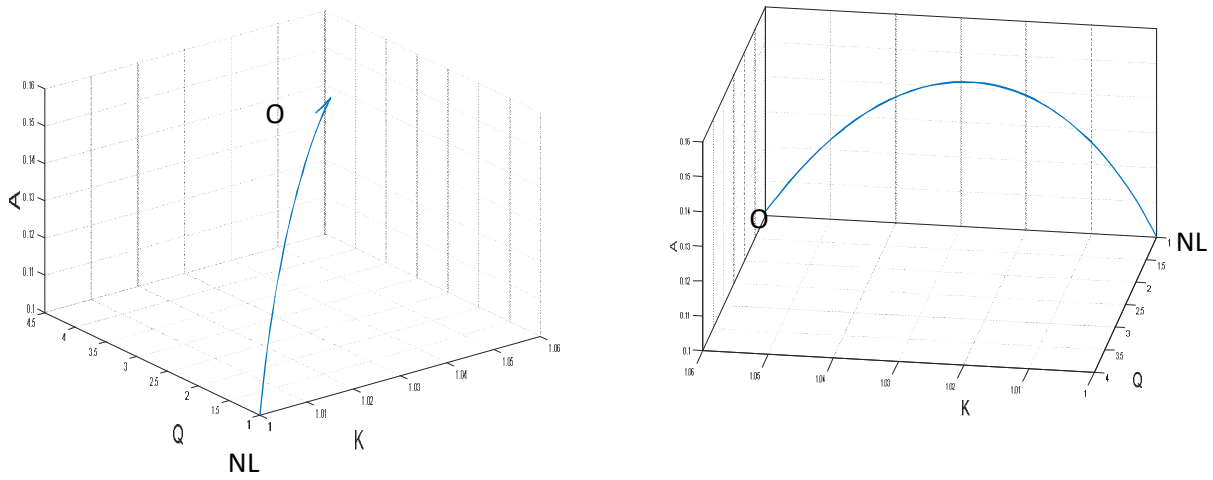

(a) (b)

Fig.2.4: Cavity soliton solution line in AQK space where all the parameters are same as Fig.2.3. (a) & (b) are in two different orientations.

2.3 CS WITH GRAPHENE AS A SATURABLE ABSORBER (GSA) WITH DELAYED FEEDBACK:

Now, we use graphene as a saturable absorber in CGLE equation with delayed feedback as :-

$$\partial_t A = \left(\beta + \frac{\iota}{2}\right)\partial_{xx}A + \delta A + \alpha_{ns}A + (\epsilon + \iota)g|A|^2A + (\mu + \omega)g^2|A|^4A + \eta e^{\iota\psi}A(x, t-\tau) \quad (13)$$

Now by following same steps as in above equation we get equation as follows

$$\partial_t A = \left(\beta + \frac{\iota}{2}\right)\partial_{XX} + (\delta + \alpha_{ns})A + (\epsilon + \iota)g|A|^2A + (\mu + \iota\nu)g^2|A|^4A + \eta e^{\iota\psi}A(x, t-\tau)$$

Let us start with the case of stationary structures where the field envelope depends on the evolution variable harmonically:-

Put $A = Fexp(-\iota\alpha t)$

$$\frac{\partial}{\partial t}(Fe^{-\iota\alpha t}) = \left(\beta + \frac{\iota}{2}\right)\frac{\partial^2}{\partial x^2}(Fe^{-\iota\alpha t}) + (\delta + \alpha_{ns})Fe^{-\iota\alpha t} + (\epsilon + \iota)g|Fe^{-\iota\alpha t}|^2 Fe^{-\iota\alpha t}$$

$$+ (\mu + \iota\nu)g^2|Fe^{-\iota\alpha t}|^4 Fe^{-\iota\alpha t} + \eta e^{\iota\psi}Fe^{-\iota\alpha t}(x, t-\tau)$$

Further solving we get

$$e^{-\iota\alpha t} = F\iota\alpha + \left(\beta + \frac{\iota}{2}\right)\partial_{xx}Fe^{-\iota\alpha t} + \delta(Fe^{-\iota\alpha t}) + \alpha_{ns}Fe^{-\iota\alpha t} + (\epsilon + \iota)g|F|^2 Fe^{-\iota\alpha t}$$

$$+ (\mu + \iota\nu)g^2|F|^4 Fe^{-\iota\alpha t} + \eta e^{\iota\psi}Fe^{-\iota\alpha t}(x, t-\tau)$$

Now take $e^{-\iota\alpha t}$, part common and cancel out from both sides

$$\left(\beta + \frac{\iota}{2}\right)\partial_{xx}F = F\iota\alpha + \delta F + \alpha_{ns}F + (\epsilon + \iota)g|F|^2 F + (\mu + \iota\nu)g^2|F|^4 F + \eta e^{\iota\psi}F(x, t-\tau) = 0$$

$$(2\beta + \iota)\frac{d^2F}{dr^2} + \frac{(D-1)}{r}\frac{dF}{dr}(2\beta + \iota)$$

$$+ 2F\left[\iota\alpha + \delta + \alpha_{ns} + (\epsilon + \iota)g|F|^2 + (\mu + \iota\nu)g^2|F|^4 + \eta e^{\iota\psi}(x, t-\tau)\right] = 0$$

Put values of $\frac{d^2F}{dr^2}$ *and* $\frac{dF}{dr}$ *in above equation then*

$$(2\beta + \iota)\left[\frac{d^2A}{dr^2}e^{\iota\phi_0} + 2\iota e^{\iota\phi_0}\frac{dA}{dr}\frac{d\phi}{dr} - Ae^{\iota\phi_0}\left(\frac{d\phi}{dr}\right)^2 + \iota Ae^{\iota\phi_0}\frac{d^2\phi_0}{dr^2}\right] + 2Ae^{\iota\phi_0}\left[\iota\alpha + \delta + \alpha_{ns} + \right.$$

$$\left.(\epsilon + \iota)gA^2 + (\mu + \iota\nu)g^2A^4 + \eta e^{\iota\psi}(x, t-\tau)\right] \quad (14)$$

Now, separate out real and imaginary parts,

$$2\beta\frac{d^2A}{dr^2} - 2A\frac{dA}{dr}\frac{d\phi}{dr} - 2A\beta\left(\frac{d\phi}{dr}\right)^2 - A\frac{d^2\phi}{dr^2} + \frac{(D-1)}{r}\left[\frac{dA}{dr}(2\beta) - A\frac{d\phi}{dr}\right] + 2A\left[\delta + \alpha_{ns} + \epsilon A^2 g + \right.$$

$$\left.\mu g^2A^4 + Re\left[\eta e^{\iota\psi}(x, t-\tau)\right]\right] = 0 \quad (15)$$

And $4\beta\frac{dA}{dr}\frac{d\phi}{dr}+\frac{d^2A}{dr^2}+2\beta A\beta\frac{d^2\phi_0}{dr^2}-A\left(\frac{d\phi}{dr}\right)^2+\frac{(D-1)}{r}\left[\frac{dA}{dr}+2\beta A\frac{d\phi}{dr}\right]+2A\left[\alpha+A^2g+\nu A^4g^2+Im\left[\eta e^{\iota\psi}(x,t-\tau)\right]\right]$ (16)

Now, put $Q=\frac{d\phi_0}{dr}, K=\frac{1}{A}\frac{dA}{dr}$

Equation 15 reduces to,

$\frac{dK}{dr}-\frac{KQ}{\beta}-Q^2-\frac{1}{2\beta}\frac{dQ}{dr}+\frac{(D-1)}{r}\left[K-\frac{Q}{2\beta}\right]+\frac{1}{\beta}\left[\delta+\alpha_{ns}+\epsilon gA^2+\mu g^2A^4+Re\left[\eta e^{\iota\psi}(x,t-\tau)\right]\right]=0$ (17)

Similarly, equation 16 reduces to,

$\frac{dK}{dr}+4\beta KQ+2\beta\frac{dQ}{dr}-Q^2+\frac{(D-1)}{r}[K+2\beta Q]+2\left[\alpha+A^2g+\nu g^2A^4+Im\left[\eta e^{\iota\psi}(x,t-\tau)\right]\right]$ (18)

Now add and subtract equations 17 and 18 we get two ordinary differential equations as such:-

$$\frac{dK}{dr}=Q^2-\frac{(D-1)(K)}{r}-\frac{2}{\left(2\beta+\frac{1}{2\beta}\right)}[\delta+\alpha_{ns}+\epsilon A^2g+\mu A^4g+\eta cos(\psi-\omega\tau]$$

$$+\frac{1}{\beta\left(2\beta+\frac{1}{2\beta}\right)}[\alpha+A^2g+\nu g^2A^4+\eta sin(\psi-\omega\tau)]$$

And

$\frac{dQ}{dr}=-2KQ-\frac{(D-1)Q}{r}+\frac{2}{4\beta^2+1}[\delta+\alpha_{ns}+\epsilon gA^2+\mu g^2A^4+\eta\cos(\psi-\omega\tau)]+\frac{4\beta}{(4\beta^2+1)}[\alpha+A^2g+\nu g^2A^4+\eta\sin(\psi-\omega\tau)]$

Further solving this equation we get three ordinary differential equations as:-

$$\frac{dA}{dr} = KA \tag{19}$$

$$\frac{dK}{dr} = Q^2 - \frac{(D-1)K}{r} - \frac{2}{\left(2\beta+\frac{1}{2\beta}\right)}[\delta + \alpha_{ns} + \epsilon A^2 g + \mu A^4 g^2 + \eta\cos(\psi - \omega\tau)] + \frac{1}{\beta(2\beta+\frac{1}{2\beta})}[\alpha +$$

$$A^2 g + \upsilon g^2 A^4 + \eta\sin(\psi - \omega\tau)] \tag{20}$$

$$\frac{dQ}{dr} = -2KQ - \frac{(D-1)Q}{r} + \frac{2}{(4\beta^2+1)}[\delta + \alpha_{ns} + \epsilon g A^2 + \mu g^2 A^4 + \eta\cos(\psi - \omega\tau)] + \frac{4\beta}{(4\beta^2+1)}[\alpha +$$

$$A^2 g + \upsilon g^2 A^4 + \eta\sin(\psi - \omega\tau)] \tag{21}$$

Now, we solve the above three coupled differential equations by Range- Kutta method (i.e., numerically). The result is described in the following paragraphs.

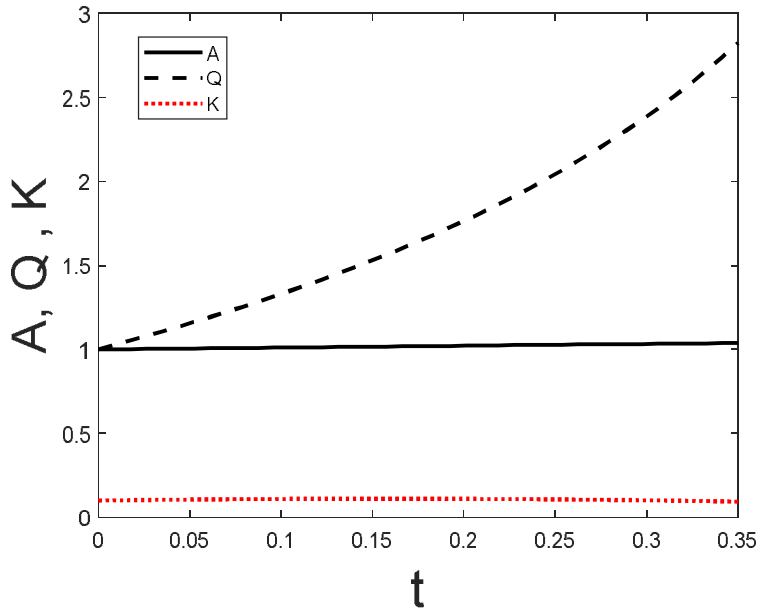

Fig.2.5: Evolution of A, K and Q where parameters are β=6.2, α=0.7, $\alpha_{ns} = 5, \epsilon = 4.0,$ *μ=2, δ=0.51, v=-0.1,* $g = 0.4$*, η=0.2, ψ=3.17, ω=9, τ=3.*

Evolution of real amplitude(A), rate of change of real amplitude (K) and the rate of change of phase (Q) with t is presented in fig.2.5. A And K remain constant while Q increases with$t$. This

indicates the formation of a structure of constant amplitude but of changing phase. It can be considered as a CS if its three major properties (mentioned earlier) are satisfied. The phase change has been further reduced in this case. The corresponding CS solution in AQK phase space is given in Fig. 2.6. This, as before, indicates the center as well as nonlasing region for the CS.

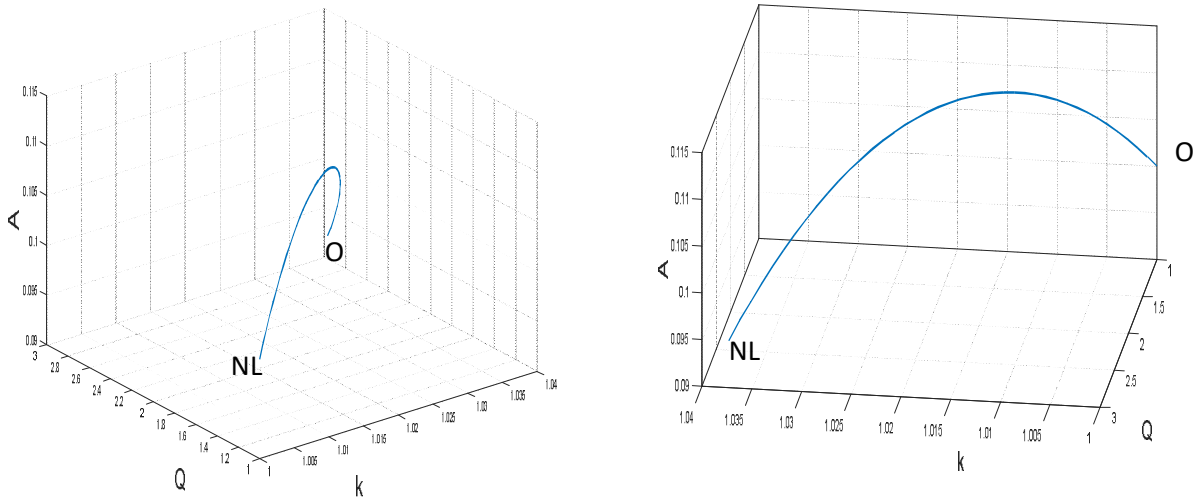

(a) (b)

Fig.2.6: Cavity soliton solution line in AQK space where all the parameters are same as Fig.2.5. (a) & (b) are in two different orientations.

2.4 CS WITH GRAPHENE AS A SATURABLE ABSORBER (GSA) WITHOUT DELAYED FEEDBACK:-

In this case, we take delayed term (τ) is zero and rest all equation remains same then we get solutions as shown below.

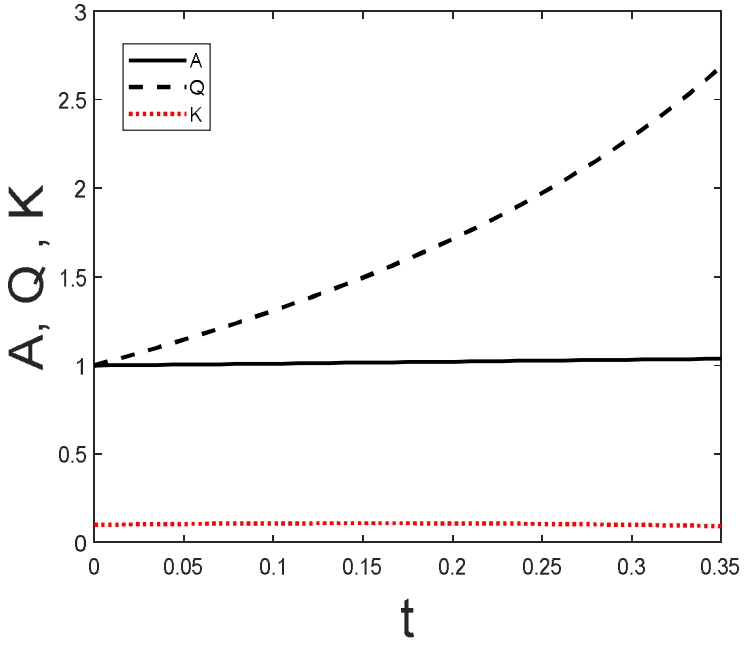

Fig.2.7: Evolution of A, Q and K where all parameters remains same except τ i.e., β=6.2, α=0.7, $\alpha_{ns} = 5$, $\epsilon = 4.0$, *μ=2, δ=0.51, ν=-0.1,*$g = 0.4$, *η=0.2, ψ=3.17, ω=9, τ=0.*

Evolution of real amplitude (A), rate of change of real amplitude (K) and the rate of change of phase (Q) with t is presented in fig.2.7. As before, A and K remain constant while Q increases with t. This indicate the formation of a structure of constant amplitude but of changing phase . This case the phase change is smaller than the earlier similar curve in section 2.3. The corresponding phase plot is given in Fig. 2.8 below.

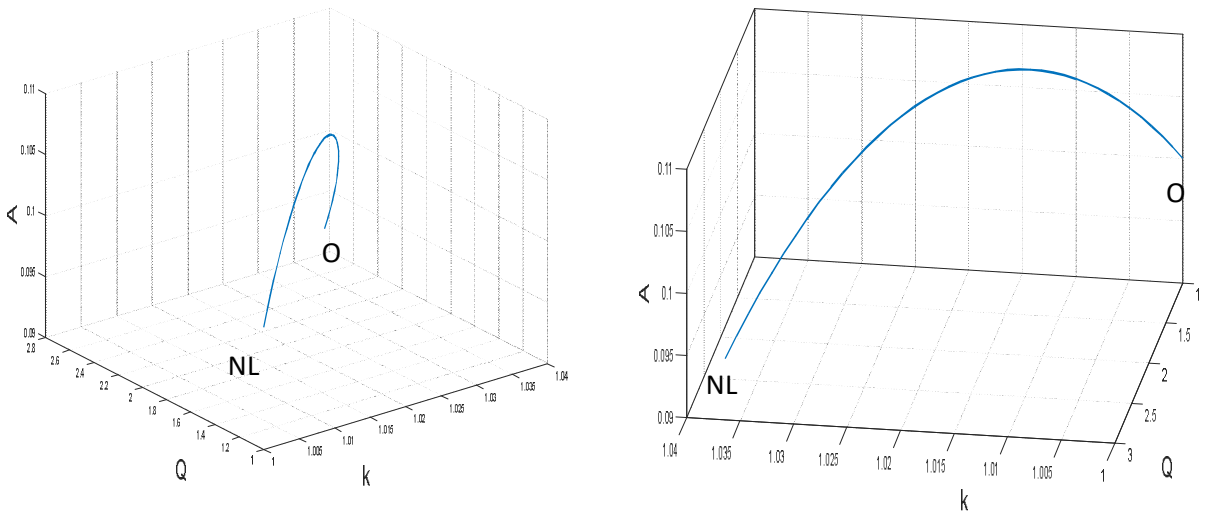

(a) (b)

Fig.2.8: Cavity soliton solution line in AQK space where all the parameters are same as Fig.2.7. (a) & (b) are in two different orientations.

2.5 PHASE PLOTS FOR DIFFERENT STRENGTHS OF GSA WITH DELAYED FEEDBACK :

We now investigate the effect of the GSA in details. We increase the saturation strength g and draw the phase plots as follows. With increasing strength of GSA the profile of the localized structure changes significantly

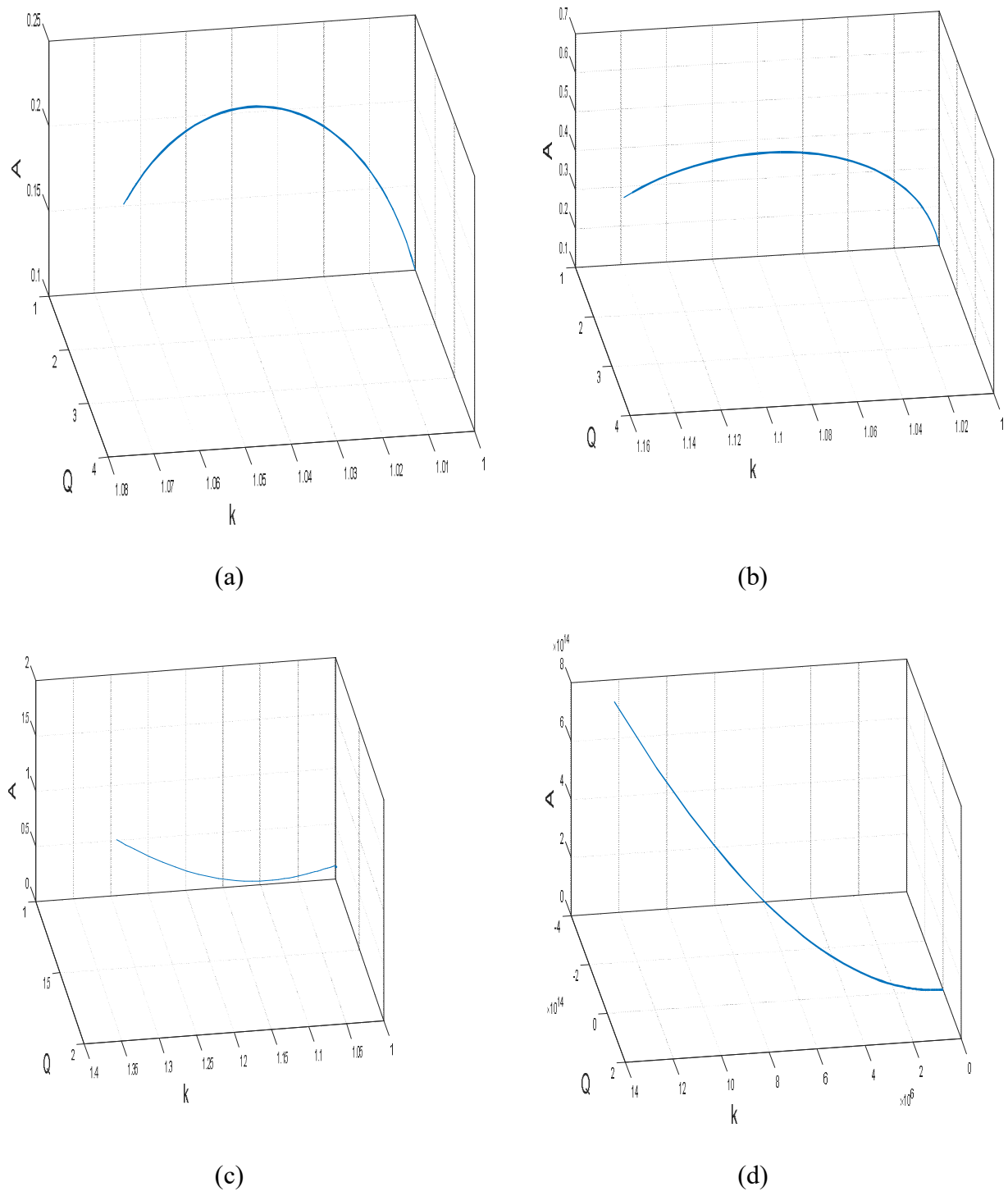

Fig.2.9: Cavity soliton solution line in AQK space where the parameters are β=6.2, α=0.7, $\alpha_{ns} = 5$ *,* $\epsilon = 4.0$*, μ=2, δ=0.51, ν=-0.1, , η=0.2, ψ=3.17, ω=9,* ***τ=3****.*

(a) $g = 1.4$*, (b)* $g = 3.4$*, (c)* $g = 4$ *and (d)* $g = 8$

2.6. PHASE PLOTS FOR DIFFERENT VALUES OF GSA WITHOUT DELAYED FEEDBACK :-

We now investigate the effect of the GSA in absence of the delay in feedback. As before, we increase the saturation strength g and draw the phase plots as follows in Fig. 2.10. Here also with increasing strength of GSA the profile of the localized structure changes significantly. The notable point is that at higher strength the curve takes large coordinate values. This was observed in the delayed feedback case too.

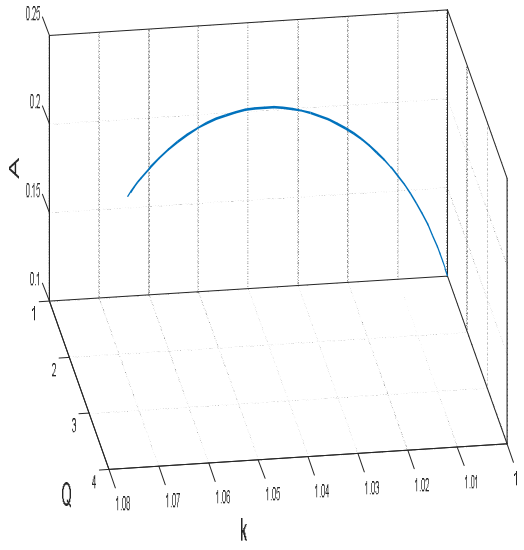

(a)

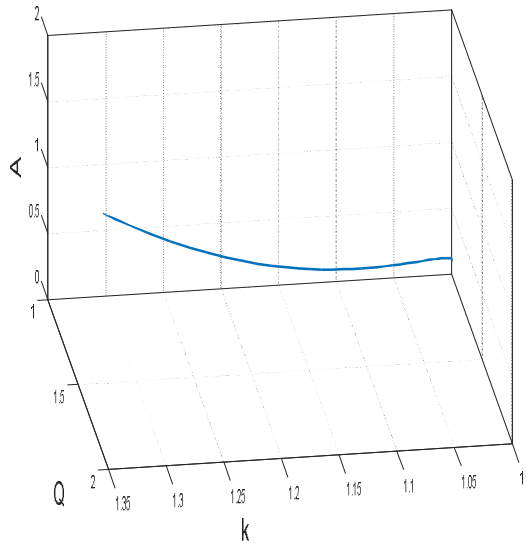

(b)

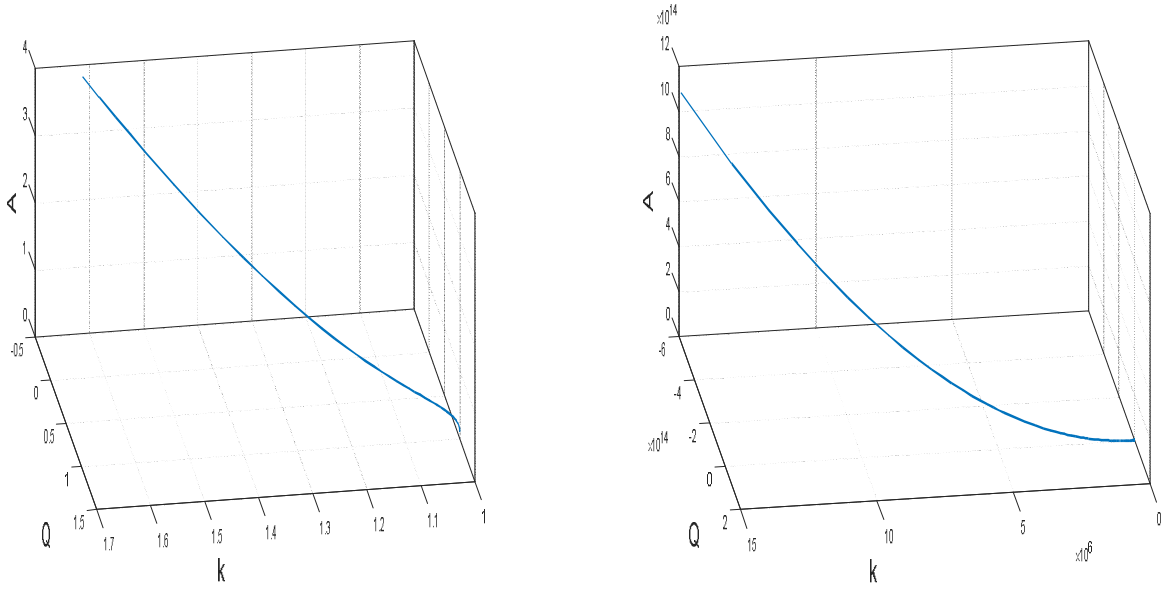

(c) (d)

Fig.2.10: Cavity soliton solution line in AQK space where the parameters are β=6.2, α=0.7, $\alpha_{ns} = 5$, $\epsilon = 4.0$, *μ=2, δ=0.51, v=-0.1,* $g = 0.4$, *η=0.2, ψ=3.17, ω=9,* ***τ=0.***

(a) $g = 1.4$, *(b)* $g = 3.4$, *(c)* $g = 4$ *and (d)* $g = 8$

2.7 PHASE PLOTS FOR DIFFERENT DELAY IN FEEDBACK WITH GSA:

Now we explore the influence of the delay in feedback on the profile of the localized structure, i.e., CS. In presence of GSA we vary, in fact, increase the delay in feedback. The *CS* solution curve in AQK space is plotted for increasing delay τ in Fig. 2.11. The profile changes significantly with the delay.

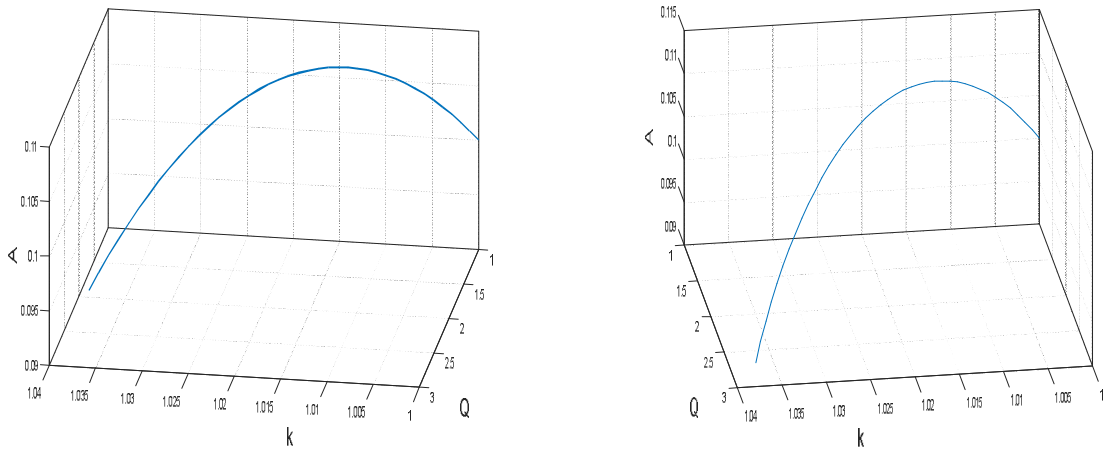

(a) (b)

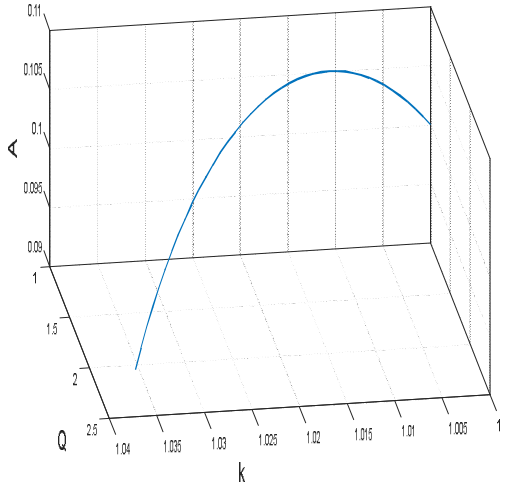

(c)

Fig.2.11: Cavity soliton solution line in AQK space where the parameters are β=6.2, α=0.7, $\alpha_{ns} = 5$, $\epsilon = 4.0$, *μ=2, δ=0.51, v=-0.1,* $g = 0.4$, *η=0.2, ψ=3.17, ω=9,*

(a) τ=4, (b) τ=8 and (c) τ=25

2.8 PHASE PLOTS FOR DIFFERENT DELAY IN FEEDBACK WITHOUT GSA:

As we explored the influence of the delay in feedback on the profile of the localized CS structure in presence of GSA, at this point it is worthy to repeat the same investigation in absence of GSA.

In this case too the CS solution curve in AQK space is plotted for increasing delayτ. Fig. 2.12 shows that the profile changes significantly with different delayed feedback.

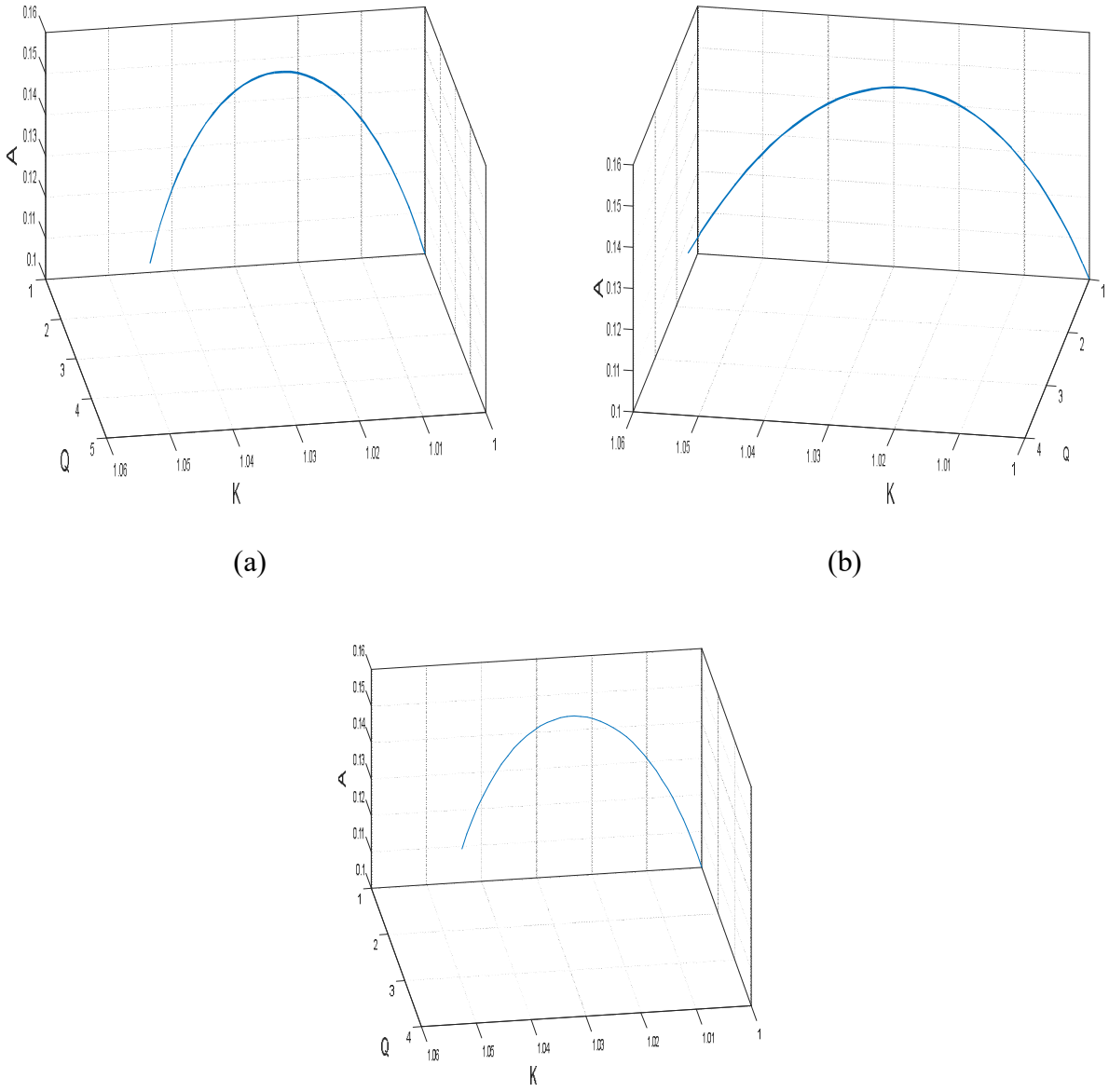

Fig.2.12: Cavity soliton solution line in AQK space with $\boldsymbol{g = 0}$. *The other parameters are* β*=6.2,* α*=0.7,* $\alpha_{ns} = 5$, $\epsilon = 4.0$, μ*=2,* δ*=0.51,* ν*=-0.1,* η*=0.2,* ψ*=3.17 and* ω*=9.*

(a) τ*=4, (b)* τ*=8 and (c)* τ*=25*

CHAPTER 3

3.1 CONCLUSION :

We determined the evolution of the localized structure in the nonlinear cvavity. If the three major properties, namely, (i) exponential localization (ii) bi-stability (iii) freedom of localization on any point on the transverse plane, are satisfied by the localized structure one can refer them as CS.We determined the evolution equations of the CS parameters for different situation of delayed feedback as well as without delay in feedback. The evolution curves show localized structure formation. However the phase cannot be constant in those structures. The 3D phase plots are generated to determine the profile of the CS. The center of the CS and the points of nonlasing state have been identified for various situations of feedback delay. We investigate all the above matters in presence and in absence of GSA. Therefore the results clearly identify the influence of graphene or GSA in the formation of CS for different feedback.

The results obtained may be of interest to the experimentalist to generate CS in laboratory environment. The influence of GSA might be a useful tool for tuning of devices that are operated based on CS. The delay in feedback can be manipulated to fabricate different optical and all-optical devices. We precisely can emphasize on the 3D imaging using the result of the present work. Delayed feedback plays an important role in 3D imaging . Imaging is based on human vision system. We human beings have binacular vision, i.e., we see any object with two eyes. The eyes are separated and each eye sees the world from the different angle. Our brain combines those different images produce the sense of depth. When we a 3D object the light from different parts of the object take different times to reach our eyes. This delay can be manipulated in 3D imaging. Our current study on delayed feedback can be aligned with the above concept of vision.

Eventually using CS, generated by delayed feedback in VCSEL, one may create a 3D imaging technique. The concept of CS may improve the 3D imaging techniques significantly.

3.2 FUTURE PLAN

One can further investigate on our CS model to explore its application in 3D sensing. Since graphene is present in the cavity, the sensing can be significantly improved, in principle. Also, other exclusive and interesting features of graphene can be used for the 3D sensing. Gesture recognition is the other related issue, which can be addressed and developed in this line.

3.3 REFERENCES :-

1. NaiL N .Akhmediev , Adrian Ankiewicz. Solitons (Nonlinear pulses and beams), **1997**.
2. S.Trillo and W. Torruellas (eds.), Spatial Solitons (springer-verlag, **2001**).
3. Y.Silberbarg, Collapse of optical pulses, opt.Lett., **1990,**15,1282.
4. N.N. Resonav, Solitons in laser systems with absorption, in: Dissipative solitons, N.Akhmediev and A.Ankiewicz eds.(Springer-Verlag, Berlin **2005**).
5. S.H.Strogatz. Nonlinear Dynamics and Chaos. Perseus Books Publishing LLC, Westview Press, **1994**.
6. N.N. Rosanov solitons in laser systems with saturable absorption,**2005**,661,101-130.
7. J.K. Hale. "Theory of functional differential equations" , NY,**1997**.
8. I.S.Aranson and L.Kramer. The world of complex Ginzburg-Landau equation.Rev.Mod.Phys.,**2002**,74,2-41.
9. Tatsushi Hamaguchi, Hiroshi Nakajima and Noriyuki Fuutagawa, GaN-based Vertical-Cavity Surface -Emitting Lasers Incorporating Dielectric Distributed Bragg Reflectors, 20feb**2019**,
10. RP Photonics, Encyclopedia.,733,1-12.
11. Blais, F.A review of 20 years of range sensors development. J. Electronic Imaging **2004**,13,231-240.
12. W.J. Firth and P.V. Paulau .Soliton lasers stabilized by coupling to a resonant linear system,**2010**,59,13-21.
13. Baldeep kaur and Soumendu Jana. Generation and dynamics of one- and two-dimensional cavity solitons in a vertical-cavity surface-emitting laser with a saturable absorber and frequency- selective feedback,**2017,**34.

14. D. Puzyrev, S. Yanchuk, A.G. Vladimirov, and S.v. Gurevich. Stability of plane wave solutions in complex Ginzburg-Landau equation with delayed feedback, **2014**, 13, 986-1009.

15. M. Tildi, A.G. Vladimirov, D. Pieroux, and D. Turaev.Spontaneous motion of cavity solitons induced by a delayed feedback, **2009**, 103, 103904.

16. Journal of Nonlinear Science, **1991-2019**,29,1432-1467.

17. Zhichao Jiang,YanfenGuo,Tongqian Zhang, Double delayed feedback control of a Nonlinear finance System, 5feb**2019**,vol.(2019), 1-17.

18. Blais, F.; Rioux, M.; Beraldin, J.A. Practical considerations for the design of a high precision 3Dlaser scanner system. *Proc. SPIE* **1988**, *959*, 225-246.

19. Baumberg, A.; Lyons, A.; Taylor, R. 3DS.O.M.-A commercial software solution to 3D scanning,Vision, Video, and Graphics (2003), The Euro- Association 2003. Eurographics Partner Event,Video, and Graphics, **2003.**

20. Levoy, M et al. The digital Michelangelo project: 3D scanning of large statues, *Proc. SIGGRAPH 00, Computer Graph. Proc., Annu. Conf. Ser.*, New Orleans, Louisiana, USA, **2000**; pp.131-144.

21. D.Puzyrev ,S.Yanchuk, A.G. Vladimirov, S.V. Gurevich.Stability of plane wave solutions in complex Ginzburg -Landau equation with delayed feedback,**2013**,1-21.

22. Qiaoliang Bao, Han Zhang, Zhenhua Ni, Yu Wang, Lakshminarayana Polavarapu, Zexiang Shen , Qing-Hua Xu, Dingyuan Tang, Kian Ping Loh, Monolyer graphene as a saturable absorber in a mode-locked laser, **2011**,4,297-307.

23. Bao, Q.; Zhang, H.; Wang, Y.; Ni, Z.; Yan, Y.; Shen, Z. X.; Loh, K. P.; Tang, D. Y. Atomic - layer graphene as a saturable absorber for ultrafast pulsed lasers. Adv. Funct. Mater. **2009**, 19, 3077-3083.

24. J.V.Moloney and A.C. Newell, Nonlinear Optics, (Addison-Wesley, Redwood City **1992**).

25. M.Tildi, E.Averlant, A.Vladimirov, K.Panajotov.Delay feedback induces a spontaneous motion of two-dimensional cavity solitons in driven semiconductor microcavities,18 sep **2012**,86,033822-8.

26. S. Shwetanshumala. Temporal solitons of modified complex Ginzburg landau equation, **2008**, 3, 17-24.

27. N.N. Rosanov, S.V. Fedorov, A.N. Shatsev.Dynamics of strong coupling formation between laser solitons, March **2004**, 98, 427-437.

28. V.V.Afanasjev, N.N.Akhmediev, and J.M. Soto-Crespo. Three forms of localized solutions of the quantic complex Ginzburg-Landau equation. Physical Review E, **1996**,53(2), 1931-1939.

29. I.S. Aranson and L. Kramer. The world of the complex Ginzburg-Landau equation. Rev. Mod. Phys.,Feb **2002**,74(1).99-143.

30. M. Lichtner, M. Wolfrum, and S.Yanchuk. The spectrum of delay differential equations with large delay. SIAM J. Math. Anal.,**2011**,43,788-802.

31. H.Broer and F.Takens. Dynamical Systems and Chaos (Applied Mathematical Sciences). Springer, New York,**2011**.

32. D.Battogtokh, A.Preuser, and A.Mikhailov. Controlling turbulence in the complex Ginzburg-Landau equation in two-dimensional systems,15 Jan **1996**,90,84-95.

33.Fuchang Yang, Z hijian Shi. Research on Static Hand Gesture Recognition Technology for Human Computer Interaction System,**2016**,92,459-463.

34.Orhan Hakki Karatas, Ebubekir Toy.Three-dimensional imaging techniques, **2014**, 8(1), 132-140.

35. Zhichao Jiang,YanfenGuo,Tongqian Zhang, Double delayed feedback control of a Nonlinear finance System, 5feb**2019**,vol.(2019), 1-17.

36. Remondino, F. From point cloud to surface: the modeling and visualization problem, *Workshopon Visualization and Animation of Reality based 3D Models*, Tarasp-Vulpera, Switzerland,February 24-28, **2003**.

37.Van Gool, L.; Zeng, G.; Van den Borre, F.; Muller, P. *Photogrammetric Image Analysis*; Stilla, U.,Mayer, H., Eds.; Institute of Photogrammetry and Cartography: Munich, Germany, September19–21, **2007**; *36*, pp. 209-220.

38.https://www.myvcsel.com/gesture-recognition-and-3d-sensing/

39.Nielsen, T.; Bormann, F.; Wolbeck, S.; Spiecker, H.; Burrows, M.D.; Andersen, P. Time-of-lightanalysis of light pulses with a temporal resolution of 100ps. *Rev. Sci. Instrum*. **1996**, *67*, 1721-1724.

40.Shiou, F. J.; Cheng, W. Y. Development of an innovative multi-detector triangulation probe. *IEEE Int. Conf. Mechatronics*, Ontario, Canada, July 24-28, **2005**; pp. 318-322.

41.Guidi, G.; Beraldin, J.-A.; Atzeni C. High accuracy 3D modeling of Cultural Heritage: the digitizing of Donatello's "Maddalena". *IEEE Trans. Image Proc.* **2004**, *13*, 370-380.

42.Anderson, S.; Levoy, M. Unwrapping and Visualizing Cuneiform Tablets. *IEEE Comput. Graph*. **2002**, *22*, 82-88.

43.Bruschweiler, W.; Braun, M.; Dirnhofer R. Analysis of patterned injuries and injury-causing instruments with forensic 3D/CAD supported photogrammetry (FPHG): an instruction manual for the documentation process. *Forensic Sci. Int.* **2003**, *132*, 130-138.

44.Altschuler, B.; Monson, K. Initial progress in the recording of crime scene simulations using 3Dlaser structured light imagery techniques for law enforcement and forensic applications. In *Proc.SPIE*, San Diego, CA, USA, July **1998**; *3240*, pp. 230-241.

45. Srinivasan, V.; Liu, H.C.; Halioua, M. Automated phase-measuring profilometry of 3-D diffuse objects. *Appl. Opt.* **1984**, *23*, 3105-3108.

46. https://www.sciencelearn.org.nz/videos/6-how-we-see-3d

47.https://wonderopolis.org/wonder/how-does-3d-work

48.https://www.myvcsel.com/gesture-recognition-and-3d-sensing/

49.Blais, F.A review of 20 years of range sensors development. J. Electronic Imaging **2004**,13,231-240.

50.Rioux, M.; Blais, F. Compact three-dimensional camera for robotics applications.J.Opt. Soc. Am.**1986**,3,1518-1521.

51.DeSouza, G.; Kak, A. Vision for Mobile Robot Navigation: A Survey. IEEE T. Pattern. Anal. **2002**,24,237-267.

Appendix-1:

The MATLAB programme for the determination of evolution of A, K and Q

```
% close all; clear all; clc;
%This programme is to solve the CGLE with delayed feedback
equations and to find the EVOLUTION PLOTS


function dydt = f(t,y);
% Declear the STEADY STATE/ EQUILIBRIUM values of the
system parameters
% As=1;Qs=1;Ks=1;
%solving the diff eqn using
[t,y] = ode45(@f,[0 0.35],[1;1;0.1]);
%Ploting of the graph
plot3(t, y(:,1),t, y(:,2),t, y(:,3),'linewidth',2);
% legend('A','Q','K')
% xlabel('t','fontsize',24);
% ylabel('A, Q , K', 'fontsize',24);
xlabel('k','fontsize',24);
ylabel('Q', 'fontsize',24);
% axis([0 2.0 0 50]);
%-----------------------------------------------------------
----------
% defining the set of Ist order differential equation.
function dydt =f(t,y)
beta=6.2;
alpha=0.7;
alpha_ns=5;
epsilon=4.0;
mu=2.0;
delta=0.51;
v=-0.1;
g1=0.4;
eta=0.2;
psi=3.17;
omega=9.*10.^(14);
tao=0;
dydt = [y(3).*y(1);
        y(2).^2-2/(2*beta+(1/2*beta)).*(delta+epsilon*(
y(1).^2)*g1+alpha_ns+...
```

```
        mu*(g1^2)*(y(1).^4)+eta.*cos(psi-
omega.*tao))+1/beta.*(2.*beta+(1/2.*beta)).*((alpha+(y(1).^
2)*g1...
        +v*(g1^2)*(y(1).^4)+eta.*sin(psi-omega.*tao)));
       -
2*y(3).*y(2)+2/(4*(beta^2)+1).*(delta+alpha_ns+epsilon*g1*(
y(1).^2)+...
       mu*(g1^2)*(y(1).^4+eta.*cos(psi-
omega.*tao)))+(4*beta./(4*(beta.^2)+1).*((alpha...

+g1.*(y(1).^2)+mu.*(g1.^2).*(y(1).^4)+eta.*sin(psi-
omega.*tao))))];
```

Appendix-2:

The MATLAB programme for the plotting of phase portrait in AQK space

```
% close all; clear all; clc;
%This programme is to solve the CGLE with delayed feedback
equations and to determine the PHASE PORTRAITS

function dydt = f(t,y);
% Declear the STEADY STATE/ EQUILIBRIUM values of the
system parameters
% As=1;Qs=1;Ks=1;
%solving the diff eqn using
[t,y] = ode45(@f,[0 0.35],[1;1;0.1]);
%Ploting of the graph
% plot(t,y(:,1),'k-',t,y(:,2),'k--
',t,y(:,3),'r:','linewidth',2);
plot3(y(:,1),y(:,2),y(:,3),'linewidth',2);
% legend('A','Q','K')
xlabel('t','fontsize',24);
ylabel('A, Q , K', 'fontsize',24);
% xlabel('k','fontsize',24);
% ylabel('Q', 'fontsize',24);
% axis([0 2.0 0 50]);
%-----------------------------------------------------------
----------
% defining the set of Ist order differential equation.
function dydt =f(t,y)
beta=6.2;
alpha=0.7;
alpha_ns=5;
epsilon=4.0;
mu=2.0;
delta=0.51;
v=-0.1;
g1=0.4;
eta=0.2;
psi=3.17;
omega=9.*10.^(14);
tao=0;
dydt = [y(3).*y(1);
        y(2).^2-2/(2*beta+(1/2*beta)).*(delta+epsilon*(
y(1).^2)*g1+alpha_ns+...
```

```
        mu*(g1^2)*(y(1).^4)+eta.*cos(psi-
omega.*tao))+1/beta.*(2.*beta+(1/2.*beta)).*((alpha+(y(1).^
2)*g1...
        +v*(g1^2)*(y(1).^4)+eta.*sin(psi-omega.*tao)));
       -
2*y(3).*y(2)+2/(4*(beta^2)+1).*(delta+alpha_ns+epsilon*g1*(
y(1).^2)+...
       mu*(g1^2)*(y(1).^4+eta.*cos(psi-
omega.*tao)))+(4*beta./(4*(beta.^2)+1).*((alpha...

+g1.*(y(1).^2)+mu.*(g1.^2).*(y(1).^4)+eta.*sin(psi-
omega.*tao))))];
```

Turnitin Originality Report

Processed on: 13-Jul-2019 11:03 +0530
ID: 1151475352
Word Count: 4871
Submitted: 1

Ramanpreet kaur thesis v02 By Ramanpreet Kaur

Similarity Index	Similarity by Source	
13%	Internet Sources:	1%
	Publications:	5%
	Student Papers:	10%

4% match (student papers from 20-Jul-2015)
Class: Thesis
Assignment: Thesis 2015
Paper ID: 556678774

2% match (student papers from 14-Jul-2017)
Class: MSc Thesis 2017
Assignment: MSc Thesis 2017
Paper ID: 830771299

1% match (publications)
Puzyrev, D., S. Yanchuk, A. G. Vladimirov, and S. V. Gurevich. "Stability of Plane Wave Solutions in Complex Ginzburg--Landau Equation with Delayed Feedback". SIAM Journal on Applied Dynamical Systems, 2014.

1% match (publications)
N.N. Rosanov. "Solitons in Laser Systems with Saturable Absorption". Lecture Notes in Physics, 2005

1% match (publications)
D. Puzyrev, A. G. Vladimirov, S. V. Gurevich, S. Yanchuk. "Modulational instability and zigzagging of dissipative solitons induced by delayed feedback". Physical Review A, 2016

1% match (student papers from 29-Jan-2018)
Class: Research Scholar Papers
Assignment: Research Scholar Papers
Paper ID: 908149634

1% match (publications)
S. Barbay. "Cavity Solitons in VCSEL Devices". Advances in Optical Technologies, 2011

< 1% match (publications)
A. H. H. Al-Masoodi, M. H. M. Ahmed, A. A. Latiff, H. Arof, S. W. Harun. "Nickel oxide nanoparticles thin film saturable absorber for 1-micron pulsed all-fibre lasers operation". Journal of Modern Optics, 2018

< 1% match (publications)
Kazuhiko Sumimura, Hidetsugu Yoshida, Hajime Okada, Hisanori Fujita, Masahiro Nakatsuka. "Suppression of self pulsing in Yb-doped fiber lasers with cooling by liquid nitrogen", 2007 Conference on Lasers and Electro-Optics - Pacific Rim, 2007

< 1% match (student papers from 13-Jan-2017)
Submitted to Koc University on 2017-01-13

< 1% match (Internet from 05-Oct-2018)
http://dlutir.dlut.edu.cn/CitedAchivement/Item/564467

< 1% match (Internet from 26-Feb-2015)
http://investorintel.com/graphite-graphene-intel/graphene-the-wonder-material-that-is-going-to-change-the-world-but-when/

< 1% match (student papers from 14-Jul-2017)
Class: MSc Thesis 2017
Assignment: MSc Thesis 2017
Paper ID: 830800292